The ikaite to calcite transformation: Implications for palaeoclimate studies

Madeleine L. Vickers [a,b,*], Martin Vickers [c], Rosalind E.M. Rickaby [d], Han Wu [e],
Stefano M. Bernasconi [f], Clemens V. Ullmann [g], Gerhard Bohrmann [h],
Robert F. Spielhagen [i], Heidemarie Kassens [i], Bo Pagh Schultz [j],
Carl Alwmark [k], Nicolas Thibault [b], Christoph Korte [b]

[a] *Centre for Earth Evolution and Dynamics (CEED), University of Oslo, P.O. Box 1028 Blindern, 0315 Oslo, Norway*
[b] *Department of Geosciences and Natural Resource Management, University of Copenhagen, Øster Voldgade 10, 1350 Copenhagen K, Denmark*
[c] *Department of Chemistry, UCL, 20 Gordon Street, London WC1H 0AJ, UK*
[d] *Department of Earth Sciences, University of Oxford, South Parks Road, Oxford OX1 3AN, UK*
[e] *Department of Chemical Engineering, UCL, Torrington Place, London WC1E 7JE, UK*
[f] *Geologisches Institut, Departement Erdwissenschaften, ETH Zürich, Sonneggstrasse 5, 8092 Zürich, Switzerland*
[g] *Cambourne School of Mines, University of Exeter, Penryn Campus, Penryn TR10 9FE, UK*
[h] *MARUM, Center for Marine Environmental Sciences and Faculty of Geosciences, University of Bremen,
Leobener Str. 8, 28359 Bremen, Germany*
[i] *GEOMAR, Helmholtz Centre for Ocean Research Kiel, Wischhofstraße 1-3, 24148 Kiel, Germany*
[j] *Museum Salling, Fur Museum, Nederby 28, 7884 Fur, Denmark*
[k] *Department of Geology, Lund University, Solvegatan 12, SE-223 62 Lund, Sweden*

Abstract

Marine sedimentary ikaite is the parent mineral to glendonite, stellate pseudomorphs found throughout the geological record which are most usually composed of calcite. Ikaite is known to be metastable at earth surface temperatures and pressures, readily breaking down to more stable carbonate polymorphs when exposed to warm (ambient) conditions. Yet the process of transformation of ikaite to calcite is not well understood, and there is an ongoing debate as to the palaeoclimatic significance of glendonites in the geological record. This study uses a combination of techniques to examine the breakdown of ikaite to calcite, outside of the ikaite growth medium, and to assess the palaeoclimatic and palaeoenvironmental significance of stable and clumped isotope compositions of ikaite-derived calcite. Powder X-ray diffraction shows that ikaite undergoes a quasi- solid-state transformation to calcite during heating of samples in air, yet when ikaite transforms under a high temperature differential, minor dissolution-recrystallisation may also occur with the ikaite structural waters. No significant isotopic equilibration to transformation temperature is observed in the resulting calcite. Therefore, in cases of transformation of ikaite in air, clumped and stable isotope thermometry can be used to reconstruct ikaite growth temperatures. In the case of ancient glendonites, where transformation of the ikaite occurred in contact with the interstitial waters of the host sediments over unknown timescales, it is uncertain whether the reconstructed clumped isotope temperatures reflect ikaite crystallisation or its transformation temperatures. Yet clumped and stable isotope thermometry may still be used conservatively to estimate an upper limit for bottom water temperatures.

Furthermore, stable isotope along with element/Ca ratios shed light on the chemical environment of ikaite growth. Our data indicate that a range of (bio)geochemical processes may act to promote ikaite formation at different marine sedimentary sites, including bacterial sulphate reduction and anaerobic oxidation of methane. The colours of the ikaites, from light brown

* Corresponding author.

to dark brown, indicate a high organic matter content, favouring high rates of bacterial sulphate reduction as the main driver of ikaite precipitation. Highest Mg/Ca ratios are found in the most unstable ikaites, indicating that Mg acts to destabilise ikaite structure.

1. INTRODUCTION

Ikaite is a rare, metastable form of hydrated calcium carbonate ($CaCO_3 \cdot 6H_2O$) that may be synthesised under certain physical and chemical conditions, and is found naturally occurring in a range of different environments (e.g. Council and Bennett, 1993; Pauly, 1963; Suess et al., 1982; Zhou et al., 2015). As recently shown in the review by Schultz et al. (2022), natural ikaite growth sites vary widely in their chemical conditions, including saline lakes and fjords (where it forms tufa towers; Pauly, 1963; Shearman et al., 1989; Bischoff et al., 1993; Council and Bennett, 1993; Buchardt et al., 2001; Omelon et al., 2001; Seaman et al., 2022); cold saline spring waters (Ito, 1996); Antarctic sea-ice (Dieckmann et al., 2008, 2010; Hu et al., 2014); the carapaces of frozen shrimp (Mikkelsen et al., 1999); brine washed-rind cheese (Tansman et al., 2017) and marine sediments (up to 10 m below the sediment–water interface; e.g. Boggs, 1972; Greinert and Derkachev, 2004; Jansen et al., 1987; Lu et al., 2012; Stein and Smith, 1985; Suess et al., 1982; Zhou et al., 2015). These sites are all characterised by having low temperatures (≤ 7 °C) and unusual chemical conditions (e.g. Abid et al., 2015; Bell et al., 2016; Buchardt et al., 2001; Huggett et al., 2005; Omelon et al., 2001; Suess et al., 1982; Whiticar and Suess, 1998; Zhou et al., 2015). The aqueous chemical conditions vary, but all are believed to feature high alkalinity in combination with chemical inhibitors of the thermodynamically more stable anhydrous carbonate polymorphs, calcite, aragonite, and/or vaterite. No single chemical inhibitor has been found to be critical, as shown by laboratory experiments that attempted to replicate environmental conditions for natural ikaite growth (e.g. Hu et al., 2014; Stockmann et al., 2018; Tollefsen et al., 2018). Such studies have suggested various factors, alone or in combination, govern ikaite stabilisation, including aqueous Mg/Ca ratios, phosphate or sulphate concentrations, salinity, or pH of the growth solution (Bischoff et al., 1993; Buchardt et al., 2001; Hu et al., 2014; Larsen, 1994; Purgstaller et al., 2017; Rickaby et al., 2006; Stockmann et al., 2018; Swainson and Hammond, 2001; Tollefsen et al., 2018; Tollefsen et al., 2020; Whiticar and Suess, 1998). Furthermore, although in nature, ikaite has only been found in environments with temperatures ranging from -2 to $+7$ °C (e.g. Buchardt et al., 2001; Hu et al., 2014; Huggett et al., 2005; Suess et al., 1982; Zhou et al., 2015), inorganic laboratory experiments have successfully synthesised and stabilised ikaite at temperatures as high as 15 °C (Stockmann et al., 2018), and have even nucleated ikaite at temperatures of up to 35 °C (Tollefsen et al., 2020).

Ikaite (both natural and synthetic) is observed to decompose to a mixture of calcite and water, possibly via other carbonate phases, when left at ambient (c. 10 – 30 °C) temperature for several hours (Marland, 1975; Stein and Smith, 1985; Jansen et al., 1987; Shaikh, 1990; Schubert et al., 1997; Whiticar and Suess, 1998; Buchardt et al., 2001; Dahl and Buchardt, 2006; Rickaby et al., 2006; Tang et al., 2009; Tollefsen et al., 2020). Different studies suggest different upper temperature limits for ikaite stability (e.g. Bischoff et al., 1993; Buchardt et al., 2001; Marland, 1975; Purgstaller et al., 2017; Stockmann et al., 2018; Tollefsen et al., 2020). Such studies imply that the chemistry of the medium in which the ikaite is stored, and/or the length of time it is kept, may be controlling factors on its breakdown temperature (e.g. Bischoff et al., 1993; Lennie et al., 2004; Purgstaller et al., 2017; Tollefsen et al., 2020). However, to date there are no studies that attempt to separate and quantify these parameters, and this may be important for understanding whether calcitic glendonites act as reliable temperature indicators in the geological record (e.g. Vickers et al., 2020).

In nature, ikaite is most commonly found growing below the sediment–water interface in continental shelf settings (e.g. Greinert and Derkachev, 2004; Jansen et al., 1987; Lu et al., 2012; Stein and Smith, 1985; Suess et al., 1982; Zabel and Schulz, 2001; Zhou et al., 2015). In such marine sedimentary settings, ikaite precipitation appears to be facilitated by high levels of bacterial sulphate reduction fuelled by high amounts of sedimentary organic matter or by anaerobic oxidation of methane (AOM). Evidence for this comes from the location of the Ikaite Formation Zone (IFZ) in seafloor sediments (Zhou et al., 2015); proximity to methane cold seeps (Greinert and Derkachev, 2004; Qu et al., 2017; Hiruta and Matsumoto, 2021); measured $\delta^{13}C$ signiatures of both modern ikaites and ancient glendonites (summarised by Vickers et al., 2018; Rogov et al., 2021), gas inclusions in glendonites (Morales et al., 2017); and glendonite biomarker signatures (Qu et al., 2017; Vickers et al., 2020).

The thermal and chemical conditions at which marine sedimentary ikaite is stable is of interest for palaeoclimate and palaeoenvironmental studies, since pseudomorphs after such ikaite (known as "glendonites") are found in the sedimentary record throughout geological time. Glendonites have traditionally been used as indicators of cold climates, both due to their frequent association with glacial sediments, and because ikaite was believed to only form at low temperatures (e.g. De Lurio and Frakes, 1999; Kemper, 1987; Kemper and Schmitz, 1981; Rogov et al., 2017; Spielhagen and Tripati, 2009). In modern marine

Table 1
Collection site locality details for the ikaites analysed in this study. *In situ* temperatures as reported by Zhou et al. (2015). Bottom water temperatures modelled using CMEMS global model (GLORYS12; https://doi.org/10.48670/moi-00021).

Ikaite location		Lat/long	Water depth (m)	depth below s-w interface (m)	*in situ* temperature (IFZ) (°C)	bottom water temperature (modelled)	collection
Bransfield Strait	Antarctic Peninsula	62°23′S, 57° 53′W	1950	20.5 to 71.4	−1.5	−2 to −0.4	Nathaniel B Palmer (NBP07)
Congo Fan	Offshore Africa	05°59.6′ S, 09°56.6′ E	3040– 4000	6.7 to 16.42	2.5 to 3.5	1.6 to 2.3	GeoB 4914–3
South Georgia	Annenkov Trough W	54°23.2′ S, 37°30.8′ W	359	5.7		−0.5 to 2.5	Cruise M134 S Georgia
Nankai Trough	Japan Trench	31°50′N, 133°51′E	6900	4.3		1.1. to 1.2	core GeoB16423-1
Laptev Sea	Siberia	78°04.5′N, 133°35.9′E	204	2.32 to 2.38		−1.6 to −0.4	ARCTIC'93 exped, Core PS2460-4

sedimentary settings where ikaite growth has been documented, *in situ* temperatures at the seafloor are below 4 °C (e.g. Greinert and Derkachev, 2004; Whiticar and Suess, 1998; Zhou et al., 2015; cf. Table 1). However, the use of glendonite as a cold-climate indicator is a matter of debate, essentially for the following four reasons: (1) the successful synthesis of laboratory ikaite at higher temperatures, suggesting that natural ikaite could have formed under warm climate conditions (Purgstaller et al., 2017; Stockmann et al., 2018; Tollefsen et al., 2020). (2) Despite a clear high-latitude/bipolar distribution of ikaite and glendonite throughout the Phanerozoic, the recent compilation of Rogov et al. (2021) still points to the rare occurrence of ancient glendonites at mid- to low- latitudes that remains to be explained. (3) Glendonites commonly occur throughout Greenhouse intervals (Rogov et al., 2021). (4) No glendonite has ever been found in sediments of the end-Ordovician glaciation nor that of the end-Devonian (Rogov et al., 2021).

It is the intention of this study to address point (1), by assessing the thermal stability and geochemistry of natural marine ikaites using the same or similar laboratory methods as those used for examining the growth and transformation of synthetic ikaite (i.e. out of their growth environment and under earth surface pressures). We apply palaeothermometry techniques on laboratory-transformed ikaites in order to assess which temperatures pseudomorphs after ikaite may preserve – ikaite growth temperatures, or transformation temperatures. We use the elemental and stable isotope signatures of the ikaites to speculate on the chemical conditions under which they grew.

2. MATERIALS AND METHODS

2.1. Ikaite collection sites

The ikaites used in this study were collected from five marine sedimentary sites across the globe (Fig. 1 and Table 1). These sites span polar to equatorial latitudes and water depths from hundreds to thousands of metres. All the sites are observed to have *in situ* bottom water temperatures in the range of −2 to + 3 °C, and temperatures in the zone of ikaite formation (IFZ) of < 4 °C, at those sites

where this data was recorded (Fig. 1 and Table 1). The ikaite samples, upon collection, were removed from the sediment and fluids in which they grew, and immediately frozen (<−15 °C) to avoid breakdown following equilibration to ambient temperature.

2.2. Sample preparation

Samples of ikaite (removed from their growth sediments and fluids) were prepared for PXRD, DSC and TGA by grinding them in a pestle and mortar partly immersed in liquid N_2 in an insulated cold-box.

2.3. Powder X-ray Diffraction

Powder X-ray Diffraction (PXRD) was used to interrogate breakdown temperatures and determine the nature of the transformation from ikaite to calcite. The instrument used was a Stoe StadiP transmission diffractometer with a copper anode at 30 mA, 40 kV and a germanium 111 monochromator to produce Kα1 X-rays. The diffracted beam was collected by an 18° 2θ Dectris Mythen1K silicon strip detector. Machine alignment was monitored using an NBS silicon standard.

For *in situ* variable temperature scans, samples were mounted in the cold-box in 0.7 mm diameter borosilicate glass capillaries and transferred to the pre-cooled diffractometer stage with an Oxford Instruments Cryojet providing a continuous controlled flow of nitrogen gas. Each series of scans was done in 1 °C steps from a start temperature between − 6 °C to 0 °C to an end temperature of between 25 °C and 30 °C, depending on machine time available. The total duration of each temperature step (including the scan) was approximately 20 min. Each data set was scanned from 10 to 60° 2θ stepping at 0.5° and 10 s/step. The resultant raw data has a step of 0.015° 2θ. To improve counting statistics and reduce possible large crystallite effects, the sample was continuously rotated in the X-ray beam.

Subsamples of freeze-box powdered Congo Fan and Laptev Sea ikaites were stored in a refrigerator and maintained at a temperature range of 2 – 4 °C. After several weeks, these were re-powdered in the cold-box and analysed
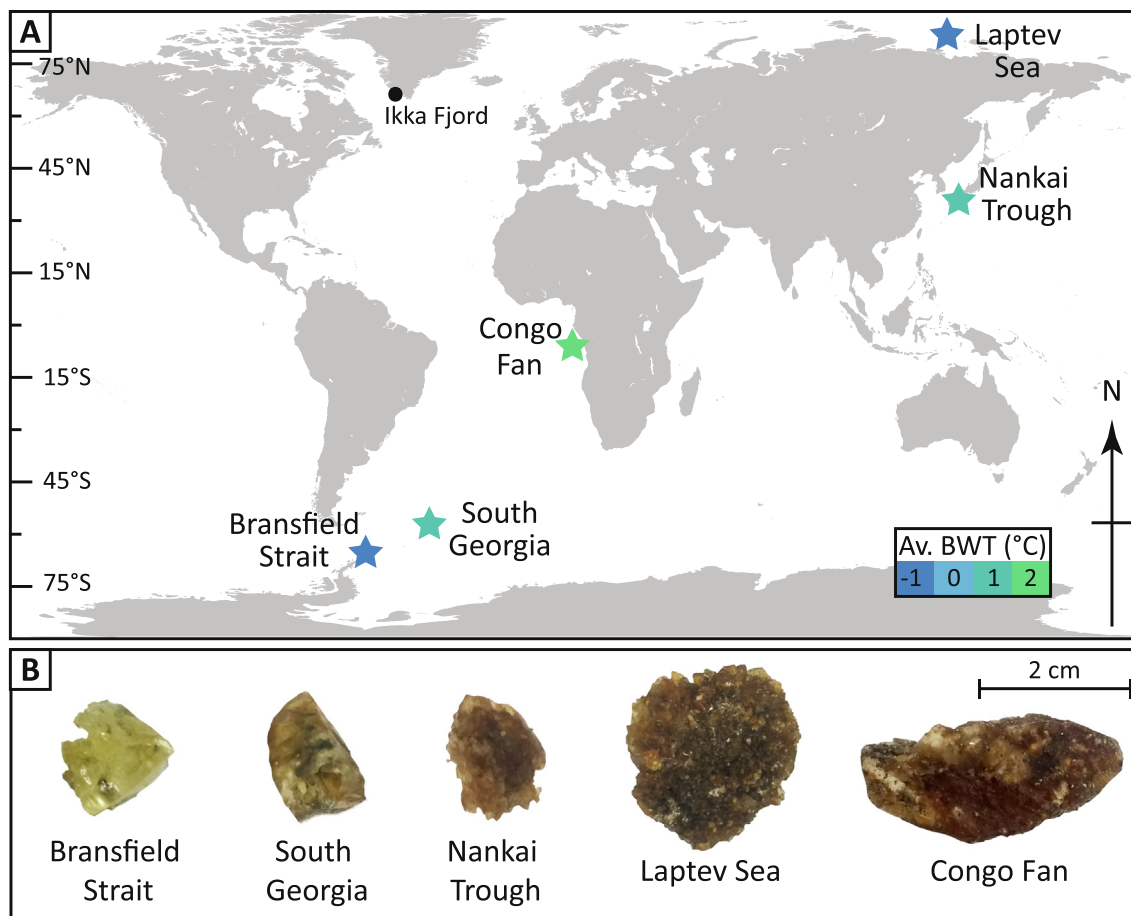
Fig. 1. **Map and photographs of the ikaites used or discussed in this study. (A)** Map showing the collection sites for the ikaites used in this study. *In situ* average annual bottom water temperatures (BWT) indicated. **(B)** Photographs of the ikaites taken from each site.

at ambient temperature. Data for these were collected quickly at 5 s/step, relying on ikaite's hysteresis to maintain phase proportions. Rather than mounting in a capillary, they were sandwiched between acetate foils to speed up the sample preparation and save alignment time.

Quantitative analysis was done using the Rietveld program "Profil" (Cockcroft, 2019). It was largely modelled on a two-phase system of ikaite and calcite, though the Nankai Trough samples had detectable quantities of an analogous calcite with a slight but significantly smaller unit-cell, so this was included as a third phase using the calcite model. The respective peaks of each of these phases were sufficiently separate to avoid correlation during refinement. Nankai Trough sample 1 additionally had a small amount of vaterite, the peaks of which were omitted from the refinements, as were occasional small peaks from the presence of ice. Throughout the refinements, atomic positions and thermal parameters of atoms in all phases remained fixed and only the scale, unit-cell, peak shape and zero offset allowed to vary. The background of each diffraction pattern was fitted graphically by eye. Input, output, fit, background, data files and graphical plots are provided in the SI.

2.4. Differential Scanning Calorimetry

Differential Scanning Calorimetry (DSC) is a technique that allows the detection of phase changes by measuring the amount of heat absorbed or released during such changes, although it cannot determine the mineralogy of the phases. DSC measures the difference in the amount of heat required to increase the temperature of a powdered sample and reference as a function of temperature. When the sample undergoes a physical transformation such as a phase transition, more or less heat is required to flow into it than the reference to maintain both at the same temperature. In this study, DSC analysis was carried out with a double furnace DSC8000 (Perkin Elmer) at Centre for Nature Inspired Engineering, CNIE Facility, UCL, in order to assess the temperature of the ikaite phase changes during breakdown under a rapid rate of heating. The DSC8000 is equipped with a dual-stage, closed-loop circulating heat exchanger IntraCooler II for sub-ambient temperature control. It also has a unique double-furnace setup, whereby the sample and the reference materials are placed in two identical furnaces. When an exothermic or endothermic event occurs in the sample, power is applied or removed from the sample

calorimeter to compensate for the change in energy. The amount of power to maintain system equilibrium is directly proportional to the energy changes occurring in the sample. This means that this DSC is very sensitive to detect thermal changes. The method was applied in order to examine the temperature at which the ikaite phase change occurred, and to compare to that observed using PXRD. The heating rates are very different between the two methods, and the temperature is more accurately constrained in the DSC compared to the PXRD with Cryojet.

Samples were transferred rapidly to the DSC pans and weighed on Sartorius Cubis-II MCA125S-2S00-I semi-micro balance before loading to the DSC instrument to avoid ikaite breakdown. The DSC was taken from $-6\,°C$ to $100\,°C$ with a heating rate of $20\,°C/min$ under the flow of N_2 gas.

2.5. Thermogravimetric analysis

Thermogravimetric analysis (TGA) measures the mass of a sample over time as the temperature changes from ambient to a set temperature, and was used to determine the % weight loss by water evaporation following ikaite breakdown, and to compare to hypothetical values as expected by molar ratios of water to $CaCO_3$ in the ikaite molecule ($CaCO_3 \cdot 6H_2O$). TGA was carried out using a Perkin Elmer Pyris1 TGA at CNIE Facility, UCL, with a standard furnace (25–1000 °C) and heated at a rate of 20 °C/min.

2.6. Scanning Electron Microscopy

A Tescan Mira3 High Resolution Schottky Field Emission (FEG-SEM) fitted with both standard and in-lens secondary electron, as well as back-scattered electron detectors at Lund University was used to observe ikaite transformation in order to further constrain the nature of the transformation. Uncoated samples of ikaite, taken from the freezer, were mounted on stubs at ambient temperature (c. 21 °C) and were run in the SEM under low vacuum mode at a pressure of 60 Pa, with no additional temperature regulation. The acceleration voltage was set to 15 kV and the working distance varied between 5 and 15 mm.

2.7. Inductively Coupled Plasma-Mass Spectrometry

Analyses of the chemical elements Fe, Mg, Mn, Cu, Al, Ca, Sr, Ba, Zn, Cd, Li and U, were undertaken on the dried ikaite-derived calcite powders in ordered to assess which, if any, showed correlation with ikaite breakdown temperatures. ICP-MS analysis was carried out using a PerkinElmer NexION 350D Inductively Coupled Plasma Mass Spectrometer (ICP-MS), at the University of Oxford. This used a PerkinElmer Micromist nebuliser, with a Quartz cyclonic spray chamber at ambient temperature (ca 20 °C). The plasma gas flow rate was 18 L/min and the nebulizer gas flow rate was 0.9–1.0 L/min. With the exception of Cd, Li and U all of the measurements were conducted using either helium or ammonia cell gases, to reduce polyatomic interferences by either kinetic energy discrimination (KED) or dynamic reaction cell (DRC) processes, respectively.

The instrument was coupled with an Elemental Scientific prepFAST M5 autosampler, which provided automated external calibrations, where the concentrations for the measured sample set were interpolated from linear regressions generated from the raw counts per second data from the series of standards. All blanks, standards and samples were diluted using 2 % HNO_3 and doped with Rh, In, Ir and Re internal standards to normalise for any instrument drift.

For quality control purposes the certified reference material (CRM): SLRS-6- river water standard from NRC Canada, was measured in conjunction with the samples and their concentrations evaluated against their certified values.

2.8. Inductively Coupled Plasma Optical Emission Spectrometry

Minor element analyses were carried out in order to directly compare the ikaites to glendonites and other diagenetic carbonates (analysed on the same instrument), and to assess if there was any correlation between S/Ca and P/Ca ratios and ikaite stability. The minor element analyses were performed using an Agilent 5110 VDV ICP-OES at the Camborne School of Mines, University of Exeter, following the method detailed in Ullmann et al. (2020). The minor element data are expressed as ratios to Ca, and calibrated using certified single element standards mixed to match the chemical composition of the analysed samples. Precision and accuracy of the analyses were measured and controlled by interspersing multiple measurements of international reference materials, JLs-1 and AK, and quality control solution (BCQ2).

2.9. Clumped Isotope Thermometry

Subsamples of Congo Fan, Bransfield Strait and Laptev Sea ikaites were powdered in the cold-box and immediately placed in a refrigerator maintained at 2 – 4 °C. These were allowed to fully transform in the refrigerator (the Laptev Sea sample took several months; the Congo Fan sample weeks, and the Bransfield Strait sample days). Once fully transformed to calcite (as determined by PXRD), the powders were dried at ambient temperature (21 °C). Subsamples of Nankai Trough, Congo Fan, South Georgia and Bransfield Strait ikaites were left to both transform and dry at ambient temperature after powdering in the cold-box. The dried transformed ikaite powders (now calcite) were analysed at ETH Zurich using a ThermoFisher Scientific MAT253 mass spectrometer coupled to a Kiel IV carbonate preparation device, following the methods described in Müller et al. (2017). The Kiel IV device included a PoraPakQ trap kept at −40 °C to eliminate potential organic contaminants. Samples were measured between 26th October and 11th of November 2020 by measuring maximum three replicates of each sample per measuring session which consists generally of 24 samples of 100–120 µg interspersed with 5 replicates each the carbonate standards ETH-1, ETH-2 and 10 replicates of ETH-3 (Bernasconi et al., 2018; Bernasconi et al., 2021). The samples were analysed in LIDI mode with 400 s of integration of sample and ref-

erence gas. All calculations and corrections were done with the software Easotope (John and Bowen, 2016). The clumped isotope data are reported on the InterCarb carbon dioxide equilibration scale I-CDES (Bernasconi et al., 2021). Temperatures were calculated using the Anderson et al. (2021) calibration. Carbon and oxygen isotope compositions are reported in the conventional delta notation with respect to VPDB.

3. RESULTS

3.1. Powder X-ray Diffraction

The ikaite samples showed a broad variability in their breakdown temperatures, both between samples and depending on the rate at which they were brought up to higher temperatures from below freezing.

All measured ikaite samples transformed to calcite, with no other crystalline carbonate polymorphs observed, even as interim phases, that were not already present before breakdown began (Fig. 2 and Supplementary Material). There is no evidence of vaterite forming as either a final product or an intermediate phase, although some vaterite was present with the Nankai Trough ikaite before breakdown.

Ikaites from the Laptev Sea (Siberia) and South Georgia showed highest (17 °C) and lowest (−2 °C) temperatures, respectively, at which the phase change began, with the other ikaites falling in between this range (Fig. 3). The

breakdown was not instantaneous and took place over timescales of minutes to hours for the different ikaites, corresponding to a temperature range of 8 to 22 °C (Fig. 3). The ikaite unit cell volumes showed a normal linear growth trend with heating, whereas the calcite showed sigmoidal unit cell volume increases as the ikaite transformation progressed (Figs. 4 and 5).

The ikaites that showed the highest breakdown temperatures were subsampled after powdering in the cold-box and stored in a refrigerator. These were then powdered again in the cold-box and analysed by PXRD at 0 °C. The Congo Fan ikaite was analysed after 18 days of storage in the fridge, and was found to have transformed entirely to calcite + water (Fig. 2B). The Laptev Sea ikaite was analysed after 23 days of storage in the fridge and had only partially transformed to calcite + water (Fig. 2D). As they were scanned at ambient temperature the rapid temperature change may have skewed the quantitative results. However, for the Laptev Sea ikaite, the binary phase example, shows relative peak intensities that clearly fit the structure models. Skewing would manifest as a poor Rietveld fit with increasingly lower intensity ikaite peaks going toward high angle, correspondingly reversed for calcite.

3.2. Differential Scanning Calorimetry (DSC) and Thermogravimetric Analysis (TGA)

Several phase changes were observed in the DSC data, which appeared as peaks in the heat flow vs temperature
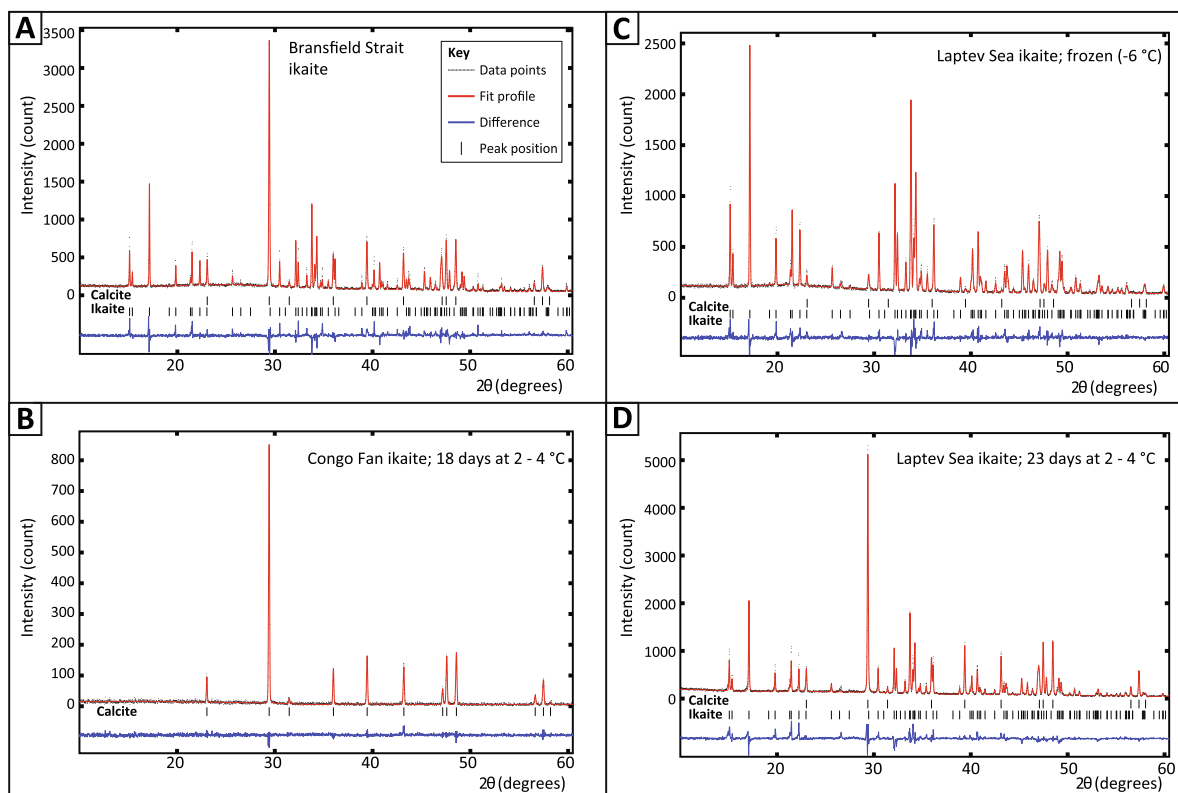

Fig. 2. **Examples of diffraction patterns for ikaite/calcite. (A)** Typical diffraction pattern for ikaite part way through transformation (Bransfield Strait ikaite, run 2, scan 6, 1 °C). **(B)** Congo fan ikaite after 18 days of refrigeration, complete transformation to calcite. **(C)** Laptev sea ikaite before breakdown (at −6 °C). **(D)** Laptev Sea ikaite after 23 days of refrigeration, showing partial breakdown to calcite (at 0 °C).
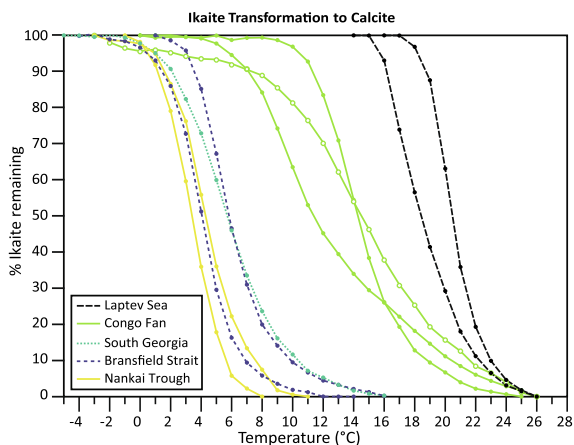
Fig. 3. **Summary of the PXRD data for ikaite transformation during progressive heating**. Here we plot the remaining % ikaite as the breakdown reaction proceeded, normalised to 100 % ikaite at the start, as some ikaites had some calcite, water ice or other phases present before breakdown began. Solid circles represent experiments run at a heating rate of 1 °C per step (at a rate of one step every 20 min); open circles indicate experimental run at a heating rate of 2 °C/step for one Congo Fan ikaite subsample.
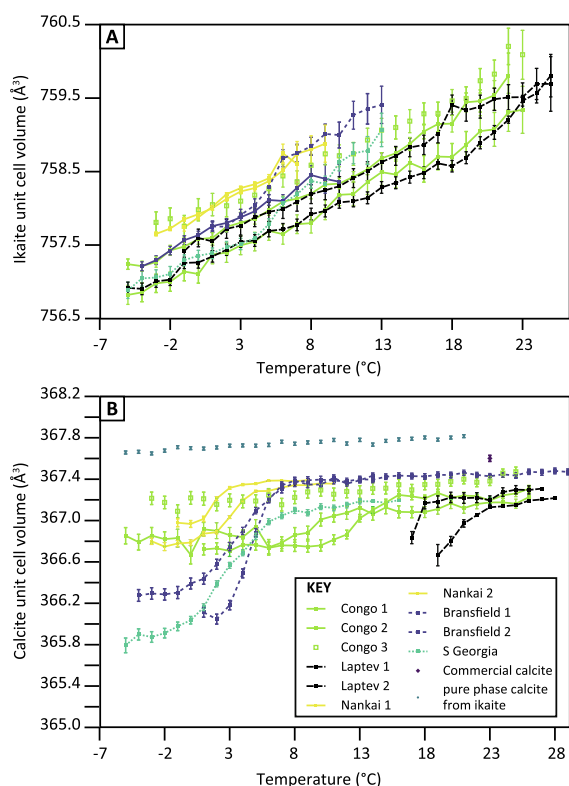

Fig. 4. **Unit cell data for the ikaites. (A)** Ikaite unit cell volumes during ikaite to calcite transformation, showing a linear thermal expansion trend. **(B)** Calcite unit cell volumes during ikaite to calcite transformation, showing a sigmoidal (non-linear), positive expansion of the unit cell volume. Interestingly, in some samples, after the curve flattens off the a-axis of calcite shows a slight but measurable negative thermal expansion.

plots (Fig. 6). These were associated with a) the phase transformation of (minor amounts of) solid water ice to liquid water, b) ikaite breakdown to water and calcite, and c) liquid water to water vapour at different temperatures (Fig. 6). Due to the (larger heat flow) concurrent melting of ice already present within the ikaite sample (first peak in Fig. 6), it was difficult to ascertain where the transformation of ikaite started. All five ikaites appeared to finish their second phase change at ~ 60 °C, but again, the presence of water (this time vaporising) led to difficulties in quantifying the thermal event (final peak in Fig. 6). There appears to be a rate-dependent hysteresis effect, such that the observed phase change at higher temperatures in the DSC than the PXRD is likely due to the much more rapid and controlled heating in the DSC than PXRD (DSC heating rate of 20 °C/min). There was a steady decrease in weight as the ikaite transformed to calcite and water was driven off as a vapour. The observed weight loss in the samples measured by TGA was between 39 and 47 %, and occurred as the ikaite dehydrated (Fig. 6). This is smaller than the theoretical value of 52 % for pure ikaite (as water makes up 52 wt% of pure ikaite), and this discrepancy wass likely caused by 1) unstable samples losing weight during the sample handling and loading steps before the measurement, total time < 1 min, 2) samples not being stable at the start of measurement, evidenced the observation of continuous loss of weight before heating started (Fig. 6). This was not shown by the TGA result as we bypassed the 1 min holding at 25 °C (common practice in TGA tests to achieve equilibrium) to avoid more sample loss during the holding step.

3.3. Scanning Electron Microscopy

SEM photomicrographs of transforming South Georgia ikaite show that the ikaite underwent very little change in the first 30 min, although the outer layer appears to bulge and flake off, sometimes revealing a pitted surface visible beneath (Fig. 7A). After nearly 2 h significant breakdown and collapse of the structure was occurring, with smaller crystals forming with space either around the outside or in the middle of the collapsed area (Fig. 7B – D).

3.4. Minor and trace element ratios

All ikaites show low element/Ca ratios compared to other diagenetic carbonates, similar to or lower than biotic carbonates (Fig. 8). The highest Mn/Ca, Fe/Ca, and Al/Ca ratios, and lowest Mg/Ca ratios are found in the most stable ikaites (Fig. 9).

3.5. Clumped and stable isotopes

The three ikaites that transformed in the fridge (c. 2 – 4 °C) returned clumped isotopic temperatures in the range of c. 0 to 4 (±3) °C (Fig. 10). The ikaites left to transform at room temperature (21 °C) gave clumped isotope temperatures ranging from c. 2 to 5 (±3) °C (Fig. 10). We note for those ikaites where one subsample transformed in the fridge and one at room temperature, the clumped temperatures are within error of each other (Fig. 10).
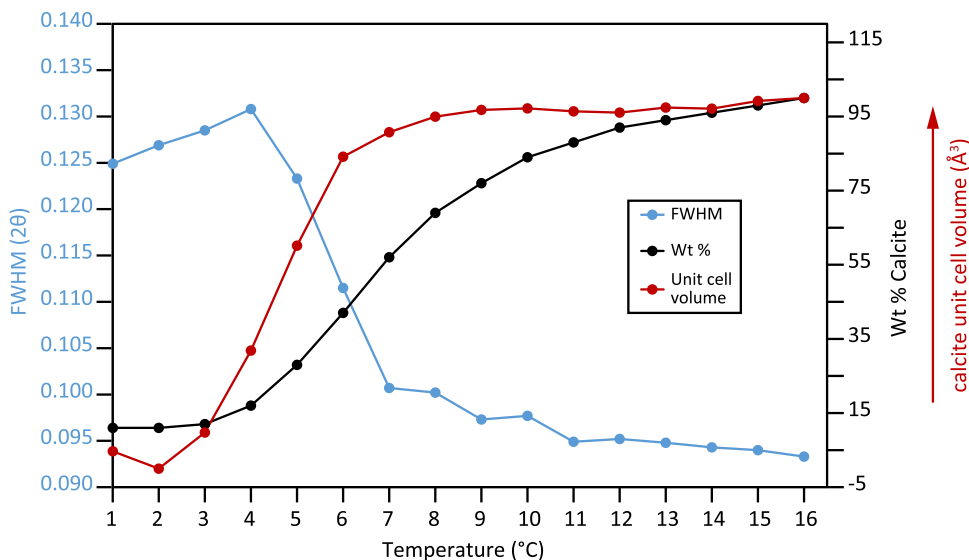
Fig. 5. **Relationship between calcite unit cell, peak width and weight %.** Example using Bransfield Strait ikaite. Peak sharpness indicated by FWHM (Full Width Half Maximum) relates to crystallite size with narrower peaks representing larger crystallites. This shows a clear correlation between crystallite size, unit cell size and abundance.
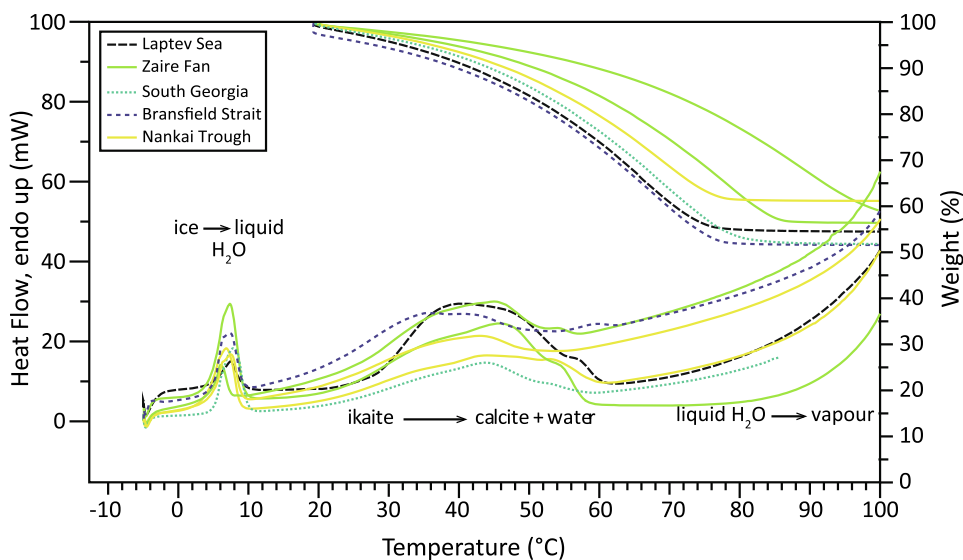

Fig. 6. **DSC and TGA data for the measured ikaites.** Left hand side shows heat flow against temperature, whereby peaks represent phase changes, and are labelled with which phase change they indicate. Right hand side (upper lines) plots the weight loss during the TGA scan against sample temperature. Only the data up to 100 °C is shown as the weight did not significantly decrease after 100 °C.

The stable isotope measurements for the transformed ikaites (now calcite) range from −0.8 to + 2.6 ‰ (VPDB) for $\delta^{18}O$ and −27.2 to + 3.7 ‰ (VPDB) for $\delta^{13}C$ (Fig. 11).

4. DISCUSSION

4.1. Temperature of ikaite breakdown

The five different ikaites (analysed outside of their growth media) showed a great variability in breakdown temperatures, both between different ikaite samples and, within a given ikaite, at different temperatures depending

on the rate of heating from sub-zero temperatures (Figs. 3 and 6). The faster the heating rate, the higher the temperature at which the ikaites began to break down, as clearly seen between the rapid heating of the DSC and the slow heating rate using the Cryojet (Figs. 3 and 6). When the sub-zero ikaite powders were placed immediately in a refrigerator after removal from the cold-box, even the most stable ikaites were observed to eventually transform to calcite (Fig. 2). The more stable ikaites took longer to break down in the refrigerator. After 23 days, the Laptev Sea sample still contained some ikaite, whilst the Congo Fan ikaite had fully transformed (Fig. 2).
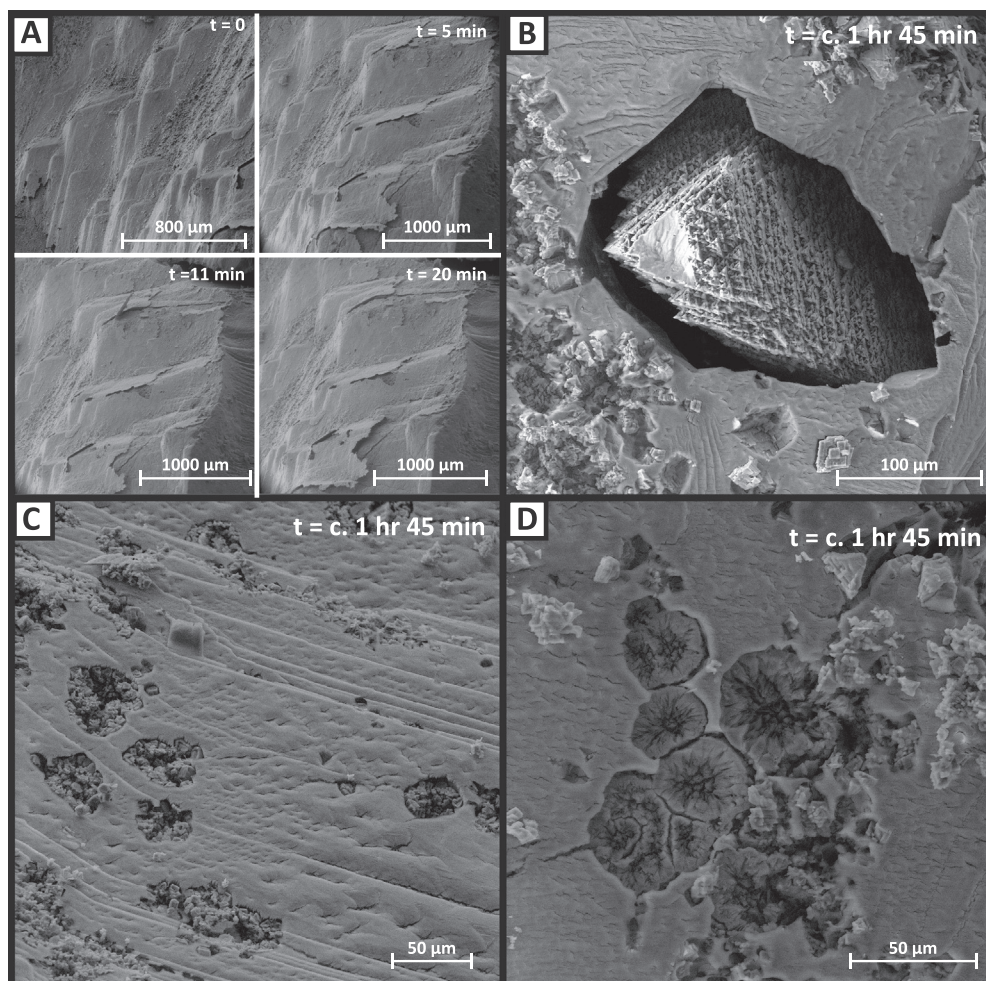
Fig. 7. Photomicrographs showing South Georgia ikaite undergoing transformation in the SEM under secondary electrons. (A) South Georgia ikaite in the first 0, 5, 11 and 20 min, showing development of flaking of the outermost layer, in some places with a pitted surface visible beneath. **(B)** Calcite formed from ikaite after 1 h 45 min, space around the new crystal due to volume difference between ikaite and calcite. **(C)** Rounded patches of decomposing ikaite. **(D)** Rounded cavities forming, texturally different from (C), possibly dissolution features.

4.2. The ikaite to calcite transformation process

The natural ikaites analysed in this study all transformed directly to calcite + water, with no intermediate polymorph $CaCO_3$ phases observed (e.g. aragonite or vaterite; Fig. 2). In the experiments of Purgstaller et al. (2017), ikaites stored in their growth solution were observed to break down to aragonite or Mg-calcite, likely due to the high Mg contents of the ikaite growth solution inhibiting calcite formation. However, when the precipitated ikaite was taken out of solution, dried at 25 ℃ and analysed by PXRD, the breakdown products were observed to be a mixture of vaterite and calcite for ikaite precipitated at 6 ℃ and just calcite for ikaite precipitated at 12 ℃ (Purgstaller et al., 2017). The PXRD studies of Shaikh (1990) and Tang et al. (2009) were undertaken on ikaite synthesized without using Mg ions in the growth solution. Shaikh (1990) allowed the ikaite to breakdown out of its growth solution, and vaterite was observed as an intermediate phase in ikaite breakdown. Tang et al. (2009) found that synthetic ikaite transformed in

its growth solution at a temperature of 37 °C, and also transformed under hot 2-propoanol (out of its growth solution), formed vaterite as an intermediate phase of ikaite breakdown. The explanation for vaterite as a breakdown product was speculated to be due to the structural arrangement of the cations and anions in ikaite being closer to that in vaterite than in calcite, so vaterite was believed to be more likely to form after dehydration (Tang et al., 2009). This implies that a solid-state transformation, rather than a dissolution-precipitation reaction, may occur, with water being evicted from the structure, leaving a hollow mesh of $CaCO_3$ that undergoes a reordering to the vaterite structure. This may then undergo transformation to calcite via either solid-state or dissolution-precipitation. Yet, other experiments on laboratory-synthesised ikaites suggest that it is the temperature at which the ikaite grew compared to that at which it transformed that determined the anhydrous carbonate phase to which it breaks down. When the temperature differential between formation and breakdown is large (e.g. > 15 ℃), vaterite was observed to form as an
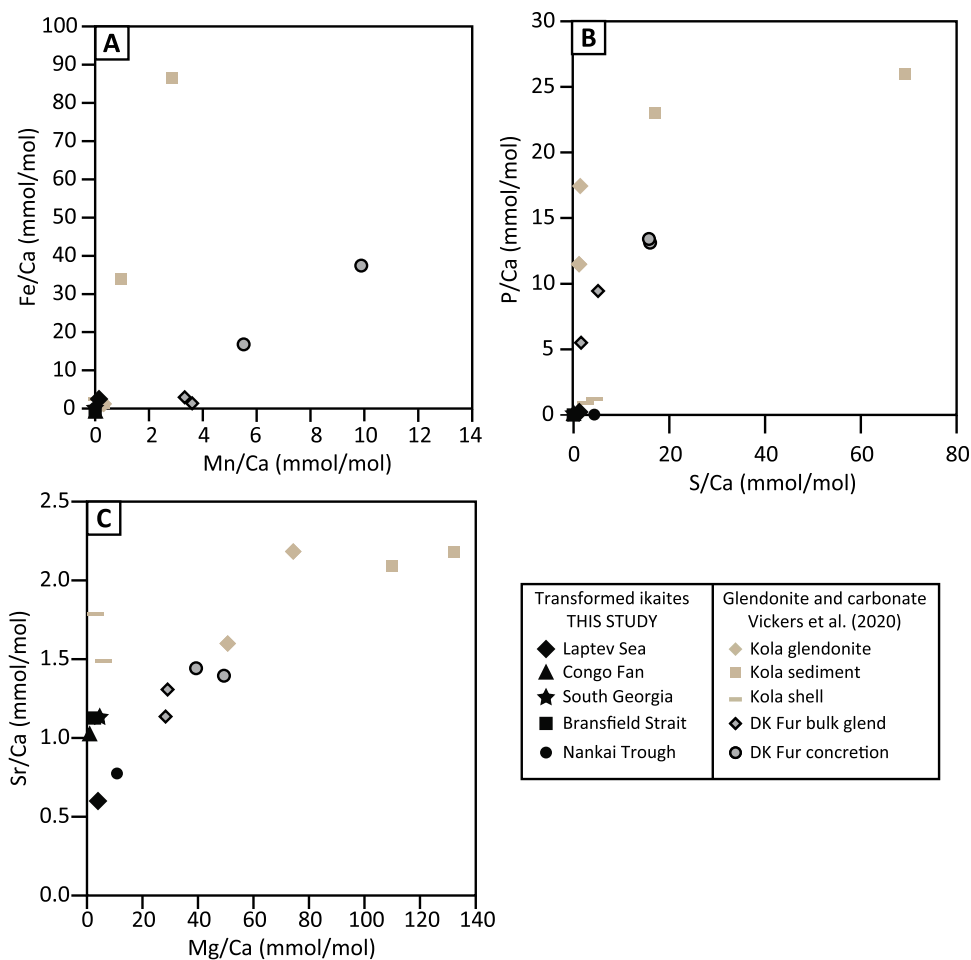
Fig. 8. **ICP-OES minor element/Ca ratios for the ikaite-derived calcites. (A), (B) and (C)** Ikaite element ratios compared to other diagenetic carbonates measured on the same instrument. Kola Peninsula and Fur Formation carbonate data from Vickers et al. (2020).
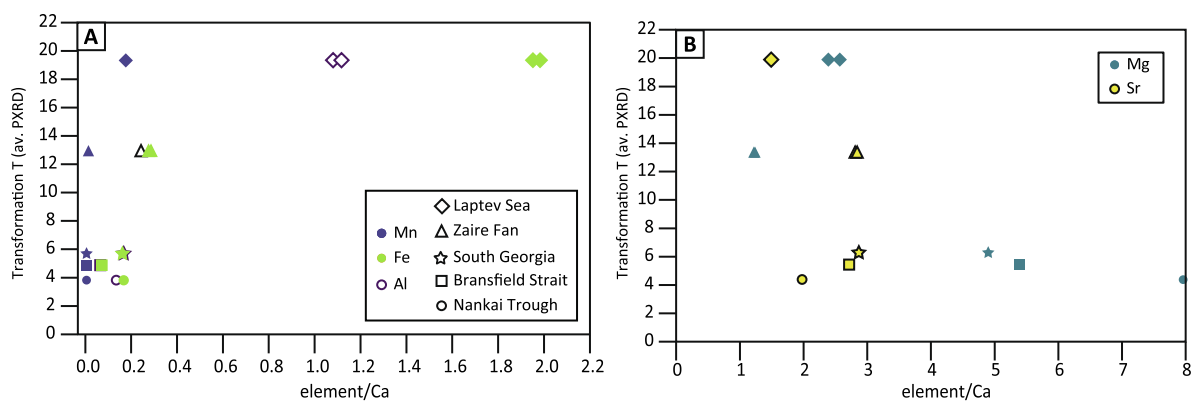

Fig. 9. **Element/Ca ratios from ICP-MS analysis of transformed and dried ikaite powders. (A)** Comparison of Mn/Ca, Fe/Ca and Al/Ca ratios with average transformation temperature. **(B)** Comparison of Mg/Ca and Sr/Ca with average ikaite transformation temperature.

intermediate stage, whereas when this differential was < 10 °C, only calcite formed (Sánchez-Pastor et al., 2016; Purgstaller et al., 2017). In our stepped heating experiments, the temperature differential was low, and therefore the observation of calcite as the only breakdown product

is in accord with the experiments of Sánchez-Pastor et al. (2016) and Purgstaller et al. (2017). Purgstaller et al. (2017) argue that almost instantaneous dissolution-reprecipitation was occurring with the adsorption of H_2O onto the ikaite crystal surface, from humidity in the
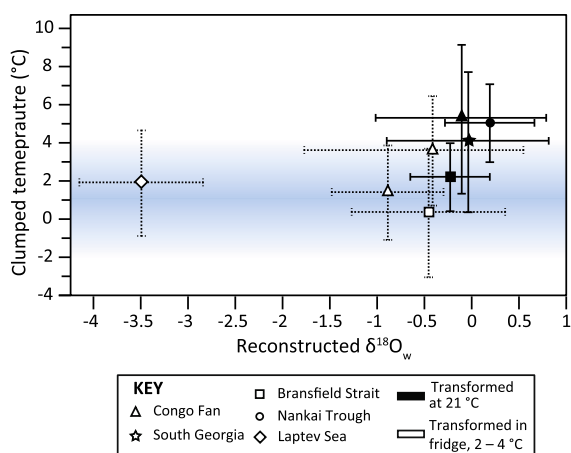
Fig. 10. **Clumped isotope temperatures and reconstructed $\delta^{18}O_w$ for the transformed ikaites.** The $\delta^{18}O_w$ was reconstructed using the equation of Kim and O'Neil (1997). Blue faded region indicates the IFZ temperature range for sites where ikaite has been recovered (Lu et al., 2012). Error bars indicate the 2σ confidence interval.

atmosphere. Tollefsen et al. (2020) further argue that the structural waters coming from the ikaite (as it breaks down) sit at the reaction interface, both when ikaite transforms in its parent solution and in air. Further examination of the textures of the subsequent breakdown products led them to agree that ikaite was undergoing a "pseudomorphic" transformation when a slight temperature/chemical differential existed, i.e. "a coupled dissolution and nucleation process within the fluid boundary layer at the parent solid surface" (Tollefsen et al., 2020 p. 7); whereas the abrupt, large change in temperature (and hypothetically other conditions e.g. chemical, Tollefsen et al., 2020) provokes (partial) dissolution and recrystallization.

In this study, the observed changing unit cell size of the calcite may suggest a quasi- solid-state transformation from ikaite to calcite, whereby the resulting and increasing charge-imbalance drives the polymerisation of (undissolved) $CaCO_3$ units. As the water exits the structure of the ikaite, the oxygens that were bound to water need to reform bonds with the calcium ions to form the calcite structure. If the water removal is progressive (as evidenced by our PXRD and SEM data and the observations of Tollefsen et al., 2020) it takes time for the structure to stabilise to the calcite configuration. Our PXRD observations show that as the ikaite transformed, the growing calcite unit cell volume was initially marginally smaller than that for commercial calcite, but increased rapidly and settled at volumes closer to commercial calcite (Fig. 4B). This was consistent with the bond lengths settling as new bonds formed, and was dominant over a true thermal effect (which would show a more linear changing unit cell size i.e. like that observed in the ikaite, Fig. 4A). We stress that the unit cell volume changes measured were very small (Fig. 4B). Initial calcite formed before and during storage was present in all samples measured; the unit cell volume of which may have been restricted by the cold storage temperatures. During PXRD heating runs, new calcite formed from ikaite, and, together with the pre-existing (storage-formed) calcite

quickly equilibrated to more stable dimensions as the ikaite finished breaking down (i.e. approaching commercial calcite; Fig. 4B). Ikaite-derived calcite left for several days to dry at room temperature showed even higher unit cell volumes (Fig. 4B).

All the ikaites measured here were collected from sites with bottom water temperatures of -2 – $+2.5$ °C, with *in situ* pore water temperatures, where these were measured, of < 3.5 °C (Table 1). The reconstructed clumped isotope temperatures for the ikaites broken down at room temperature or under refrigerated conditions are all within the expected temperature for ikaite crystallization in the IFZ (-2 to 4 °C; Zhou et al., 2015). However, although within the analytical uncertainty of each other, those ikaites transformed in the refrigerator did consistently return temperature slightly colder than those broken down at room temperature (Fig. 10). In order to alter the clumped (and oxygen) isotopic composition of the original carbonate group, the ikaite would have to fully dissolve, and the dissolved CO_3^{2-} ions undergo exchange of oxygen isotopes with the ikaite structural waters, which would require the breaking of a C—O bond and thus conversion to CO_2. Our observations of clumped isotope temperatures not reflecting the high breakdown temperatures indicate that equilibration to ambient conditions did not occur, and are consistent with both our hypothesis of quasi- solid-state transformation (i.e. whereby $CaCO_3$ units did not break), and with the "instantaneous" dissolution – precipitation model for ikaite transformation of Tollefsen et al. (2020), whereby the timescales of the transformation are too short ($<$minutes) for isotopic equilibration to occur (Guo, 2020). Our clumped isotopic findings agree with those of Rickaby et al. (2006), who precipitated synthetic ikaite in a highly alkaline solution and decomposed (cleaned) crystals out of this solution. Here, they found that the $\delta^{18}O$ for the ikaite carbonate was the same as that for the K_2CO_3 used to prepare the ikaite growth solution. The high pH (>13) of the growth solution prevented equilibration of the precipitating ikaite to the growth temperature (2 °C) (e.g. Uchikawa and Zeebe, 2012). During breakdown, there was only the ikaite structural waters present, so the lack of equilibration to ambient temperature indicates that this transformation must have been either quasi- solid-state, or below equilibration timescales for dissolution-precipitation (Uchikawa and Zeebe, 2012).

The ikaite observed to break down in the SEM did so at ambient temperature (c. 21 °C) rather than by gradual heating from frozen as in the PXRD experiments. Our SEM observations show ikaite collapsing to smaller crystals, forming a porous structure with space either around the edge or at the centre of the collapsing area (Fig. 7B & C), which fits both our hypothesis of a quasi- solid-state transformation (as evidenced by the PXRD results) and that of "pseudomorphic" transformation proposed by Tollefsen at al. (2020). However, in some areas, rounded pits formed in the surface (Fig. 7D) are possibly a dissolution-recrystallisation feature, as similar features observed by Tollefsen et al. (2020) were interpreted as such. The clumped isotope temperatures for ikaite transformed at 21 °C being marginally warmer than those transformed in
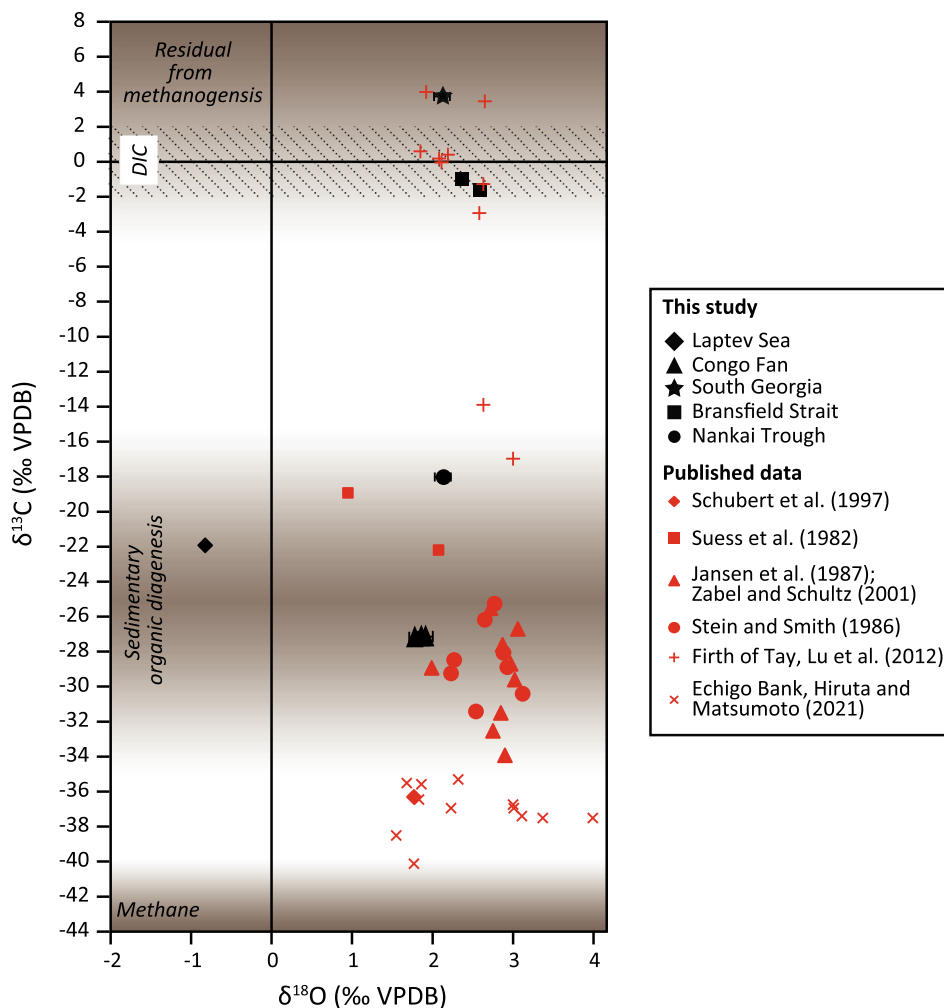
Fig. 11. **Stable isotope data for transformed ikaites.** Measured stable isotope data for dried transformed ikaite powders (this study), compared to published data for transformed ikaites from the same locations and other sites (in red; from Suess et al., 1982; Stein and Smith, 1985; Jansen et al. 1987; Schubert et al., 1997; Zabel and Schulz, 2001; Lu et al., 2012). The data in red crosses shows the measured stable isotope ratios from a single transformed ikaite (after freeze-drying) from the Echigo Bank, Sea of Japan (Hiruta and Matsumoto, 2021). Brown fade indicates the ranges of $\delta^{13}C$ for methane, sedimentary organic diagenesis and residual from methanogenesis; region in slashed dashed lines indicates range for dissolved inorganic carbon (DIC) (Campbell, 2006).

the fridge may indicate that limited isotope exchange occurred due to some small areas being fully recrystallised (Fig. 10).

4.3. Ikaite environment of formation and stability

In the marine sedimentary realm, there is evidence that bacterial sulphate reduction or the anaerobic oxidation of methane stabilises ikaite over other $CaCO_3$ polymorphs (e.g. Bischoff et al., 1993; Greinert and Derkachev, 2004; Jansen et al., 1987; Larsen, 1994; Morales et al., 2017; Qu et al., 2017; Rickaby et al., 2006; Selleck et al., 2007; Stein and Smith, 1985; Suess et al., 1982; Whiticar and Suess, 1998). It is believed that the high alkalinities, in combination with release of other calcite/aragonite inhibitors (e.g. phosphate, amino acids), as generated by these processes, promote ikaite stabilisation (e.g. Bischoff et al., 1993; Suess et al., 1982; Swainson and Hammond, 2001;

Whiticar and Suess, 1998; Zhou et al., 2015). For ikaites from a single site, there is a broad range in measured $\delta^{13}C$ (Fig. 11); and in some cases the $\delta^{13}C$ data from different studies do not appear to agree at all. Our measured $\delta^{13}C$ for the Bransfield Strait ikaite are similar to that of other ikaites from the Antarctic (e.g. from the Firth of Tay and South Georgia; this study and Lu et al., 2012) (Fig. 11); yet is apparently at odds with $\delta^{13}C$ values measured by Suess et al. (1982) for other ikaite crystals from the Bransfield Basin, and two ikaite crystals from the Firth of Tay (Lu et al., 2012) (<−14 ‰; Fig. 11). Very positive sedimentary carbonate $\delta^{13}C$ values represent the residual DIC enriched in ^{13}C by methanogenesis (−5 to + 20 ‰) (see Campbell, 2006 for a review). Some of the Antarctic ikaites show more positive $\delta^{13}C$ values than seawater DIC (−2 to + 2 ‰), suggesting that these ikaites could have incorporated carbon from the ^{13}C-enriched DIC left after methanogenesis. Those with much more negative $\delta^{13}C$

(e.g. $< -12 ‰$) could conceivably use carbon from both AOM and DIC, with the majority coming from DIC in order explain the ikaite $\delta^{13}C$ being considerably heavier than that of methane (Fig. 11), or else the majority of their carbon was derived from the decomposition of sedimentary organic matter (Campbell, 2006).

The ikaites from the other sites measured in this and previous studies (i.e. Congo Fan, Nankai Trough, Laptev Sea) all have $\delta^{13}C$ values within the range of sedimentary organic diagenesis, with none exhibiting the very positive $\delta^{13}C$ values seen in the Antarctic samples (Fig. 11). This is consistent with recent findings that ikaites from the Sea of Japan have a much heavier $\delta^{13}C$ than nearby methane-derived authigenic carbonates, indicating that the ikaites are not deriving most or all of their carbon from AOM (Hiruta and Matsumoto, 2021).

Since no significant oxygen isotope exchange with water is believed to have occurred during ikaite transformation (e.g. this study and Rickaby et al., 2006), the clumped isotope temperatures can be used in conjunction with the measured calcite $\delta^{18}O$ to reconstruct the $\delta^{18}O$ of the water from which the ikaite precipitated ($\delta^{18}O_w$), using the equation of Kim and O'Neil (1997). This equation is used because Lu et al. (2012) showed that the ikaite-water oxygen isotope fractionation for (presumably slow growing) natural marine sedimentary ikaite is comparable to that determined for synthetic calcite by Kim and O'Neil (1997). The uncertainty on the reconstructed $\delta^{18}O_w$ is large due to the relatively large confidence intervals for the clumped temperatures, yet it is in agreement with the estimated $\delta^{18}O$ of the bottom waters at these localities (Fig. 10LeGrande and Schmidt, 2006). Although the ikaites precipitated from pore waters, not bottom waters, the expected down-core variation in $\delta^{18}O$ of the pore waters is below the uncertainty range in the reconstructed $\delta^{18}O_w$ (e.g. $< 1 ‰$ for depths in the sediment of ≤ 100 m; Schrag et al., 2002; Adkins et al., 2002; Lu et al., 2012).

We expect that higher concentrations of an element in the ikaite reflects higher concentrations in the IFZ, yet it is notable that the transformed ikaites measured in this study all show very low element/Ca ratios compared to sedimentary carbonates and even aragonitic shells (Fig. 8). This indicates that the ikaite structure cannot easily accommodate other cations. Several recent studies have argued that Mg/Ca ratios in the pore waters from which the ikaite precipitates are the dominant controlling factor on ikaite stabilisation (by suppressing calcite nucleation, Purgstaller et al., 2017; Stockmann et al., 2018). We observe that the lowest Mg/Ca ratios in ikaite-derived calcite correspond to the highest breakdown temperature (Fig. 9), suggesting that Mg also acts to destabilise ikaite. This is expected, since the Mg ion is much smaller than Ca, and has a much tighter hydration sphere. Mg therefore has a destabilising effect on both ikaite and calcite, yet the effect must be stronger on calcite than ikaite, meaning that under very high Mg concentrations, ikaite may be formed preferentially compared to calcite if Ca^{2+} and CO_3^{2-} are supersaturated. This may suggest that laboratory studies that use high Mg concentrations to force precipitation of ikaite at high tempera-

tures (e.g., Purgstaller et al., 2017; Stockmann et al., 2018; Tollefsen et al., 2018) may not accurately replicate the diversity of chemical conditions in natural marine sedimentary ikaite growth sites (as already suggested by Lu et al., 2012; Vickers et al., 2019; Zhou et al., 2015).

The observation of variable colour, coupled with unclear inorganic geochemical trends, may suggest that the stability of the ikaites analysed is governed by a/multiple biological component(s) or process(es). The ikaites analysed in this study show a range of colours, which may indicate variable organic matter contents, and indeed, the darkest coloured ikaites are the most stable (Congo Fan and Laptev Sea, Fig. 1B). Whiticar and Suess (1998) suggest that the presence of amino acids in the interstitial fluid may act to stabilise ikaite in the Bransfield Strait sediments. The ikaite tufa towers which are found growing in the Ikka Fjord in Greenland (Fig. 1) appear to be strongly influenced by microbial activity, in particular through envelopment and stabilisation of the ikaite by microbial biofilms (Trampe et al., 2016). Ancient glendonites show distinct zoning defined by light and dark brown areas in thin sections, believed to be defined by organic matter inclusions (e.g. Huggett et al., 2005; Stein and Smith, 1985; Vickers et al., 2018; Vickers et al., 2020). Whilst biological analysis is beyond the scope of this study, we emphasise the need for further study to understand the role biological processes may play in marine sedimentary ikaite growth and stabilisation.

4.4. Implications for palaeoclimate studies

The few published data on ancient glendonites show that primary ikaite-derived calcites record low clumped isotope temperatures within or at the upper limit of the range for the IFZ (Zhou et al., 2015; Vickers et al., 2020). In these examples, the ikaite transformed in an aqueous setting, and it is not known whether that happened through dissolution-reprecipitation, rather than quasi- solid-state as our study suggests for conversion out of an aqueous setting. Thus, it is unclear if the clumped isotope temperatures for glendonites reflect ikaite crystallisation temperatures, preserved because either the transformation was by dissolution-precipitation but was too rapid for isotope re-equilibration, or because it was a quasi- solid-state; or if they reflect slow ikaite to calcite conversion by dissolution-precipitation in equilibrium with the pore waters at low temperatures. For glendonites, we know that the parent ikaite crystallised and transformed below the seafloor (at depths of metres to 10 s of metres; Zhou et al., 2015); and as the temperature increases with depth according to the local geothermal gradient (e.g. Zhou et al., 2015), the clumped temperatures derived from well-preserved ancient glendonites (whether preserving the ikaite growth or ikaite transformation temperature) must be warmer than bottom water temperatures. Therefore, the low temperatures derived for glendonites may be regarded as an upper limit for bottom water temperatures (e.g., Vickers et al., 2020).

5. CONCLUSIONS

This study shows that ikaite, removed from its parent medium, may undergo a quasi- solid-state transformation to calcite when temperatures are gradually raised, whereby $CaCO_3$ units previously complexed with H_2O molecules undergo polymerisation when the water gets evicted from the structure. Limited dissolution-recrystallisation within the released structural waters may also occur when the transformation process happens at ambient temperatures (21 °C). We demonstrate that the variability in the temperature of ikaite stability is a function of the rate of heating and, at least partially, linked with impurities in the ikaite crystal structure, which is in itself linked to the conditions at the site of formation (although the pressure and ambient chemical environment may play a role too). We find that magnesium incorporation into ikaite reduces ikaite stability. The carbon isotopes for four of the ikaites measured are within the range for sedimentary organic diagenesis, suggesting that the carbon was largely derived from organic matter. Yet, very positive $\delta^{13}C$ values for Antarctic ikaites imply that residual, fractionated carbon after methanogenesis was a significant carbon source for those ikaites. These findings suggest that in different settings bacterial sulphate reduction and methanogenesis/AOM may create the chemical conditions which favour ikaite precipitation.

We demonstrate that clumped isotope thermometry can be used on ikaite-derived calcites that were transformed in air to reconstruct ikaite growth temperatures. This study examined natural ikaites at surface (rather than subocean) pressures, and not within the aqueous chemical environment in which they nucleated, therefore we cannot determine if ikaite transformation in marine sedimentary settings behaves differently. Nonetheless, whether the clumped isotopic signatures of ancient glendonites reflects either ikaite crystallisation or ikaite transformation temperatures, we show that this method may be used to estimate an upper limit for bottom water temperatures.

DECLARATION OF COMPETING INTEREST

The authors declare that they have no known competing financial interests or personal relationships that could have appeared to influence the work reported in this paper.

DATA AVAILABILITY

We have shared the data as a Supplementary Materials file (Excel format) called "research data".

ACKNOWLEDGEMENTS

AUTHOR CONTRIBUTIONS

MLV designed the study, co-ran the PXRD, DSC and TGA, co-interpreted the data, and wrote the manuscript, additionally securing funding for the study.

MV ran the PXRD analysis, undertook the Rietveld analysis and made the interpretations thereof, and co-wrote the manuscript.

REMR: Co-conceived the study, provided expert knowledge and helped with the interpretation of the data; provided access to the Congo Fan and Bransfield Strait ikaites, and oversaw the running and interpretation of the ICP-MS analysis.

HW ran the TGA and DSC analysis and aided the interpretation thereof.

SMB ran and processed the clumped isotope data and co-interpreted the data.

CVU ran the ICP-OES analysis and provided the interpretation of the data.

GB Provided expert knowledge and aided interpretation of the data, and enabled access to the Nankai Trough ikaite.

RFS provided expert knowledge and aided interpretation of the data.

HK led the expedition to Russia to collect the Laptev Sea ikaites and preserved the specimens after collection.

BPS and CA undertook SEM surface imaging of ikaite breakdown.

NT helped with the interpretation of the data.

CK secured funding for this study.

APPENDIX A. SUPPLEMENTARY MATERIAL

Supplementary material to this article can be found online at https://doi.org/10.1016/j.gca.2022.08.001.

REFERENCES

Abid K., Spagnoli G., Teodoriu C. and Falcone G. (2015) Review of pressure coring systems for offshore gas hydrates research. *Und. Tech.* **33**, 19–30.

Adkins J. F., McIntyre K. and Schrag D. P. (2002) The salinity, temperature, and δ18O of the glacial deep ocean. *Science* **298**, 1769–1773.

Anderson N. T., Kelson J. R., Kele S., Daëron M., Bonifacie M., Horita J., Mackey T. J., John C. M., Kluge T., Petschnig P. and Jost A. B. (2021) A unified clumped isotope thermometer calibration (0.5–1,100 C) using carbonate-based standardization. *Geophy. Res. Lett.* **48**(7) p.e2020GL092069.

Bell J. B., Aquilina A., Woulds C., Glover A. G., Little C. T., Reid W. D., Hepburn L. E., Newton J. and Mills R. A. (2016) Geochemistry, faunal composition and trophic structure in reducing sediments on the southwest South Georgia margin. *Roy. Soc. Op. Sci.* **3** 160284.

Bernasconi Stefano M., Daëron M., Bergmann K. D., Bonifacie M., Meckler A. N., Affek H. P., Anderson N., Bajnai D., Barkan E., Beverly E. and Blamart D., et al. (2021) InterCarb: A community effort to improve interlaboratory standardization of the carbonate clumped isotope thermometer using carbonate standards. *Geochem. Geophy. Geosys.* **22**(5) p.e2020GC009588.

Bernasconi S. M., Müller I. A., Bergmann K. D., Breitenbach S. F., Fernandez A., Hodell D. A., Jaggi M., Meckler A. N., Millan I. and Ziegler M. (2018) Reducing uncertainties in carbonate clumped isotope analysis through consistent carbonate-based standardization. *Geochem. Geophy. Geosys.* **19**(9), 2895–2914.

Bischoff J. L., Fitzpatrick J. A. and Rosenbauer R. J. (1993) The Solubility and Stabilization of Ikaite (CaCO$_3$.6H$_2$O) from 0° to 25°C: Environmental and Paleoclimatic Implications for Thinolite Tufa. *J. Geo.*, 21–33.

Boggs S. (1972) Petrography ang geochemistry of rhombic, calcite pseudomorphs from mid-Tertiary mudstones of the Pacific Northwest, USA. *Sedimentology* **19**, 219–235.

Buchardt B., Israelson C., Seaman P. and Stockmann G. (2001) Ikaite tufa towers in Ikka Fjord, southwest Greenland: their formation by mixing of seawater and alkaline spring water. *J. Sed. Res.* **71**, 176–189.

Campbell K. A. (2006) Hydrocarbon seep and hydrothermal vent paleoenvironments and paleontology: Past developments and future research directions. *Palaeo., Palaeo., Palaeo.* **232**(2–4), 362–407.

Cockcroft, K.J., 2019. Powder Diffraction Program Library (PDPL), Department of Chemistry, Christopher Ingold Laboratories, London, United Kingdom, http://pd.chem.ucl.ac.uk/www/pdpl/pdpl.htm.

Council T. C. and Bennett P. C. (1993) Geochemistry of ikaite formation at Mono Lake, California: Implications for the origin of tufa mounds. *Geology* **21**, 971–974.

Dahl K. and Buchardt B. (2006) Monohydrocalcite in the arctic Ikka fjord, SW Greenland: first reported marine occurrence. *J. Sed. Res.* **76**, 460–471.

De Lurio J. L. and Frakes L. A. (1999) Glendonites as a paleoenvironmental tool: implications for early Cretaceous high latitude climates in Australia. *Geochim. Cosmochim. Acta* **63**, 1039–1048.

Dieckmann G. S., Nehrke G., Papadimitriou S., Göttlicher J., Steininger R., Kennedy H., Wolf-Gladrow D. and Thomas D. N. (2008) Calcium carbonate as ikaite crystals in Antarctic sea ice. *Geophys. Res. Lett.*, 35.

Dieckmann G., Nehrke G., Uhlig C., Göttlicher J., Gerland S., Granskog M. and Thomas D. (2010) Ikaite (CaCO$_3$. 6H$_2$O) discovered in Arctic sea ice. *Cryosphere* **4**, 227–230.

Greinert J. and Derkachev A. (2004) Glendonites and methane-derived Mg-calcites in the Sea of Okhotsk, Eastern Siberia: implications of a venting-related ikaite/glendonite formation. *Mar. Geo.* **204**, 129–144.

Guo W. (2020) Kinetic clumped isotope fractionation in the DIC-H2O-CO2 system: patterns, controls, and implications. *Geochim. Cosmochim. Acta* **268**, 230–257.

Hiruta A. and Matsumoto R. (2021) Geochemical comparison of ikaite and methane – derived authigenic carbonates recovered from Echigo Bank in the Sea of Japan. *Mar. Geo.* **443** 106672.

Hu Y.-B., Wolf-Gladrow D. A., Dieckmann G. S., Völker C. and Nehrke G. (2014) A laboratory study of ikaite (CaCO$_3$·6H$_2$O)

precipitation as a function of pH, salinity, temperature and phosphate concentration. *Mar. Chem.* **162**, 10–18.

Huggett J., Schultz B., Shearman D. and Smith A. (2005) The petrology of ikaite pseudomorphs and their diagenesis. *Proc. Geol. Assoc.* **116**, 207–220.

Ito T. (1996) Ikaite from cold spring water at Shiowakka. *Japan. J. Econ. Min. Pet.* **91**, 209–219.

Jansen J., Woensdregt C., Kooistra M. and Van Der Gaast S. (1987) Ikaite pseudomorphs in the Congo deep-sea fan: an intermediate between calcite and porous calcite. *Geology* **15**, 245–248.

John C. M. and Bowen D. (2016) Community software for challenging isotope analysis: First applications of 'Easotope' to clumped isotopes. *Rapid Commun. Mass Spect.* **30**(21), 2285–2300.

Kemper E. (1987). *Das Klima der Kreide-Zeit. Geols. Jahr.* **96**, 185.

Kemper E. and Schmitz H. H. (1981) Glendonite—Indikatoren des polarmarinen Ablagerungsmilieus. *Geols. Runds.* **70**, 759–773.

Kim S. T. and ONeil, J.R. (1997) Equilibrium and nonequilibrium oxygen isotope effects in synthetic carbonates. *Geochim. Cosmochim. Acta* **61**(16), 3461–3475.

Larsen D. (1994) Origin and paleoenvironmental significance of calcite pseudomorphs after ikaite in the Oligocene Creede Formation. *Colorado. J. Sed. Res.* **64**, 593–603.

LeGrande A. N. and Schmidt G. A. (2006) Global gridded data set of the oxygen isotopic composition in seawater. *Geophys. Res. Let.* **33**(12), 1–5.

Lennie A., Tang C. and Thompson S. (2004) The structure and thermal expansion behaviour of ikaite, CaCO$_3$· 6H$_2$O, from T= 114 to T= 293 K. *Min. Mag.* **68**, 135–146.

Lu Z., Rickaby R. E., Kennedy H., Kennedy P., Pancost R. D., Shaw S., Lennie A., Wellner J. and Anderson J. B. (2012) An ikaite record of late Holocene climate at the Antarctic Peninsula. *EPSL* **325**, 108–115.

Marland G. (1975) The stability of CaCO$_3$· 6H$_2$O (ikaite). *Geochim. Cosmochim. Acta* **39**, 83–91.

Mikkelsen A., Andersen A. B., Engelsen S. B., Hansen H., Larsen O. and Skibsted L. (1999) Presence and dehydration of ikaite, calcium carbonate hexahydrate, in frozen shrimp shell. *J. Ag. Food Chem.* **47**, 911–917.

Morales C., Rogov M., Wierzbowski H., Ershova V., Suan G., Adatte T., Föllmi K. B., Tegelaar E., Reichart G.-J. and de Lange G. J. (2017) Glendonites track methane seepage in Mesozoic polar seas. *Geology* **45**, 503–506.

Müller I. A., Fernandez A., Radke J., Van Dijk J., Bowen D., Schwieters J. and Bernasconi S. M. (2017) Carbonate clumped isotope analyses with the long-integration dual-inlet (LIDI) workflow: Scratching at the lower sample weight boundaries. *Rap. Comm. Mass Spec.* **31**, 1057–1066.

Omelon C. R., Pollard W. H. and Marion G. M. (2001) Seasonal formation of ikaite (CaCO$_3$· 6H$_2$O) in saline spring discharge at Expedition Fiord, Canadian High Arctic: Assessing conditional constraints for natural crystal growth. *Geochim. Cosmochim. Acta* **65**, 1429–1437.

Pauly H. (1963) " Ikaite", a New Mineral from Greenland. *Arctic* **16**, 263–264.

Purgstaller B., Dietzel M., Baldermann A. and Mavromatis V. (2017) Control of temperature and aqueous Mg^{2+}/Ca^{2+} ratio on the (trans-) formation of ikaite. *Geochim. Cosmochim. Acta* **217**, 128–143.

Qu Y., Teichert B., Birgel D., Goedert J. and Peckmann J. (2017) The prominent role of bacterial sulfate reduction in the formation of glendonite: a case study from Paleogene marine strata of western Washington State. *Facies* **63**, 10.

Rickaby R., Shaw S., Bennitt G., Kennedy H., Zabel M. and Lennie A. (2006) Potential of ikaite to record the evolution of oceanic δ^{18}O. *Geology* **34**, 497–500.

Rogov M. A., Ershova V. B., Shchepetova E. V., Zakharov V. A., Pokrovsky B. G. and Khudoley A. K. (2017) Earliest Cretaceous (late Berriasian) glendonites from Northeast Siberia revise the timing of initiation of transient Early Cretaceous cooling in the high latitudes. *Cret. Res.* **71**, 102–112.

Rogov M., Ershova V., Vereshchagin O., Vasileva K., Mikhailova K. and Krylov A. (2021) Database of global glendonite and ikaite records throughout the Phanerozoic. *Earth Syst. Sci. Data* **13**, 343–356.

Sánchez-Pastor N., Oehlerich M., Astilleros J. M., Kaliwoda M., Mayr C. C., Fernández-Díaz L. and Schmahl W. W. (2016) Crystallization of ikaite and its pseudomorphic transformation into calcite: Raman spectroscopy evidence. *Geochim. Cosmochim. Acta* **175**, 271–281.

Schrag D. P., Adkins J. F., McIntyre K., Alexander J. L., Hodell D. A., Charles C. D. and McManus J. F. (2002) The oxygen isotopic composition of seawater during the Last Glacial Maximum. *Quat. Sci. Rev.* **21**, 331–342.

Schubert C., Nürnberg D., Scheele N., Pauer F. and Kriews M. (1997) ^{13}C isotope depletion in ikaite crystals: evidence for methane release from the Siberian shelves? *Geo-Marine Letters* **17**, 169–174.

Schultz B., Thibault N. and Huggett J. (2022) The minerals ikaite and its pseudomorph glendonite: Historical perspective and legacies of Douglas Shearman and Alec K. *Smith. Proc. Geol. Assoc.* **133**(2), 176–192.

Seaman P., Sturkell E., Gyllencreutz R., Stockmann G. J. and Geirsson H. (2022) New multibeam mapping of the unique Ikaite columns in Ikka Fjord. *SW Greenland. Mar Geo*, 444.

Selleck B. W., Carr P. F. and Jones B. G. (2007) A review and synthesis of glendonites (pseudomorphs after ikaite) with new data: assessing applicability as recorders of ancient coldwater conditions. *J. Sed. Res.* **77**, 980–991.

Shaikh A. (1990) A new crystal growth form of vaterite, $CaCO_3$. *J. app. crys.* **23**, 263–265.

Shearman D., McGugan A., Stein C. and Smith A. (1989) Ikaite, $CaCO_3 \cdot 6H_2O$, precursor of the thinolites in the Quaternary tufas and tufa mounds of the Lahontan and Mono Lake Basins, western United States. *GSA Bull.* **101**, 913–917.

Spielhagen R. F. and Tripati A. (2009) Evidence from Svalbard for near-freezing temperatures and climate oscillations in the Arctic during the Paleocene and Eocene. *Palaeogeo., Palaeoclim Palaeoec.* **278**, 48–56.

Stein C. and Smith A. (1985) Authigenic carbonate nodules in the Nankai Trough, Site 583. *In. Rep. Deep Sea Drill. Proj.* **77**, 659–668.

Stockmann G., Tollefsen E., Skelton A., Brüchert V., Balic-Zunic T., Langhof J., Skogby H. and Karlsson A. (2018) Control of a calcite inhibitor (phosphate) and temperature on ikaite precipitation in Ikka Fjord, southwest Greenland. *App. Geochem.* **89**, 11–22.

Suess E., Balzer W., Hesse K.-F., Müller P., Ungerer C. and Wefer G. (1982) Calcium carbonate hexahydrate from organic-rich sediments of the antarctic shelf: Precursors of glendonites. *Science* **216**, 1128–1131.

Swainson I. P. and Hammond R. P. (2001) Ikaite, $CaCO_3 \cdot 6H_2O$: Cold comfort for glendonites as paleothermometers. *Am. Min.* **86**, 1530–1533.

Tang C., Thompson S., Parker J., Lennie A., Azough F. and Kato K. (2009) The ikaite-to-vaterite transformation: new evidence from diffraction and imaging. *J. Appl. Crys.* **42**, 225–233.

Tansman G. F., Kindstedt P. S. and Hughes J. M. (2017) Minerals in food: crystal structures of ikaite and struvite from bacterial smears on washed-rind cheese. *The Can. Min.* **55**, 89–100.

Tollefsen E., Stockmann G., Skelton A., Mörth C. M., Dupraz C. and Sturkell, E.,Chemical controls on ikaite formationin tollefsen,, et al. (2018) chemical controls on ikaite formation. *Min. Mag.* **82**, 1119–1129.

Tollefsen E., Balic-Zunic T., Mörth C.-M., Brüchert V., Lee C. C. and Skelton A. (2020) Ikaite nucleation at 35 °C challenges the use of glendonite as a paleotemperature indicator. *Sci. Rep.* **10**, 1–10.

Trampe E. C., Larsen J. E., Glaring M. A., Stougaard P. and Kühl M. (2016) In situ dynamics of O_2, pH, Light, and photosynthesis in Ikaite Tufa columns (Ikka Fjord, Greenland)—a unique microbial habitat. *Fron. microbio.* **7**, 722.

Uchikawa J. and Zeebe R. E. (2012) The effect of carbonic anhydrase on the kinetics and equilibrium of the oxygen isotope exchange in the CO2–H2O system: Implications for δ^{18}O vital effects in biogenic carbonates. *Geochim. Cosmochim. Acta* **95**, 15–34.

Ullmann C. V., Boyle R., Duarte L., Hesselbo S., Kasemann S., Klein T., Lenton T., Piazza V. and Aberhan M. (2020) Warm afterglow from the Toarcian Oceanic Anoxic Event drives the success of deep-adapted brachiopods. *Sci. Rep.* **10**(1), 1–11.

Vickers M. L., Price G. D., Jerrett R. M., Sutton P., Watkinson M. P. and FitzPatrick M. (2019) The duration and magnitude of Cretaceous cool events: Evidence from the northern high latitudes. *GSA Bull.* **131**, 1979–1994.

Vickers M. L., Lengger S. K., Bernasconi S. M., Thibault N., Schultz B. P., Fernandez A., Ullmann C. V., McCormack P., Bjerrum C. J. and Rasmussen J. A. (2020) Cold spells in the Nordic Seas during the early Eocene Greenhouse. *Nat. Comms.* **11**, 1–12.

Vickers M., Watkinson M., Price G. D. and Jerrett R. (2018) An improved model for the ikaite-glendonite transformation: evidence from the Lower Cretaceous of Spitsbergen, Svalbard. *Norwegian J. Geol.* **98**, 15.

Whiticar M. J. and Suess E. (1998) The Cold Carbonate Connection Between Mono Lake, California and the Bransfield Strait. *Antarctica. Aqu. Geochem.* **4**, 429–454.

Zabel M. and Schulz H. D. (2001) Importance of submarine landslides for non-steady state conditions in pore water systems—lower Congo (Congo) deep-sea fan. *Mar. Geo.* **176**, 87–99.

Zhou X., Lu Z., Rickaby R. E., Domack E. W., Wellner J. S. and Kennedy H. A. (2015) Ikaite Abundance Controlled by Porewater Phosphorus Level: Potential Links to Dust and Productivity. *J. Geo.* **123**, 269–281.

Associate editor: Weifu Guo